

Process Modeling of Storm-Water Flow in a Bioretention Cell

Zhuangxiang He¹ and Allen P. Davis, F.ASCE²

Abstract: A two-dimensional variable saturated flow model was developed to simulate subsurface flow in bioretention facilities employing the Richards' equation. Variable hydrologic performances of bioretention are evaluated using the underdrain outflow hydrographs, outflow volumes for 10 storms with various duration and depth, and flow duration curves for 25 different storms. The effects of some important design parameters and elements are tested, including media type, surrounding soils, initial water content, ratio of drainage area to bioretention surface area, and ratio of cell length to width. Model results indicate that the outflow volume via underdrain is less than the inflow; the flow peak is significantly reduced and delayed. Underdrain outflow volume from loamy sand media (with larger K_s) is larger than that from sandy clay loam media. The saturated hydraulic conductivity, storage capacity, and exfiltration into surrounding soils contribute to the hydrologic performance of a bioretention cell. Initial media storage capacity is affected by the hydraulic properties of media soils, initial water content, and bioretention surface area. The exfiltration volume is determined by the surrounding soil type and exfiltration area, dominated by flow through the bottom of the media. **DOI:** 10.1061/(ASCE)JIR.1943-4774.0000166. © 2011 American Society of Civil Engineers.

CE Database subject headings: Urban areas; Stormwater management; Runoff; Biological processes; Hydrologic models.

Author keywords: Urban storm-water runoff; Bioretention; Modeling; Hydrology; Richards' equation; Storage; Exfiltration.

Introduction

Bioretention is a low-impact development (LID) best management practice (BMP), providing a mulch/soil/plant-based trapping medium to collect, store, infiltrate, and treat urban storm-water runoff. The primary bioretention medium consists of a sand/soil/organic matter mixture with high hydraulic conductivity, which is surrounded by the native (usually less permeable) soils. A mulch layer is typically maintained on the medium surface. A vegetative layer provides evapotranspiration, pollutant uptake, and enhanced porosity of the medium. A ponding area serves as a storage reservoir, and thereafter extends the time for water to infiltrate into the medium.

Bioretention was developed to recover postdevelopment hydrology and also can improve the quality of storm-water runoff before discharge to receiving waters. Field studies have demonstrated the ability of bioretention to increase the lag time and reduce the peak flow rates as well as the total volume of surface discharge (Dietz and Clausen 2005; Hunt et al. 2006; Davis 2008; Yang et al. 2009). These net hydrologic modifications to the drainage area, attributable to evapotranspiration, ponding and media storage, and exfiltration into surrounding soil provide erosion control, flood control, and groundwater recharge. Bioretention exhibits better hydrologic performance in small storm events than in larger storms (Li et al. 2009; Brown et al. 2009). The ratio of cell media volume to drain-

age area is reported as an important factor in controlling hydrologic performance; a larger ratio and greater medium depth is expected to promote better performance (Li et al. 2009).

Current standards of bioretention design differ among various jurisdictions. For example, the state of Maryland recommends a ponding depth up to 30 cm and a soil/media mix of 50% sand, 30% topsoil, and 20% well-aged organic matter (MDE 2000), whereas the state of Delaware recommends a ponding depth up to 45 cm and a soil/media mix of 1/3 sand, 1/3 peat moss, and 1/3 mulch (DNREC 2005). Primary design elements hypothesized to affect flow control include drainage area, bioretention surface area, ponding depth, media depth and composition, underdrain configuration, surrounding soil properties, rainfall characteristics (depth, duration, and intensity), vegetation, and temperature (Davis et al. 2009). Design criteria will continue to mature with implementation of and research on bioretention. However, current bioretention performance data mainly focus on discharge from bioretention facilities. Flow processes within facilities are not clear. Limited work has been done to demonstrate the effects of primary design elements on bioretention performance.

To continue the maturation of bioretention research, comprehensive modeling ventures must be undertaken to complement ongoing experimental and monitoring programs. Only a few hydrologic models are available to simulate storm-water runoff management through bioretention. A *RECARGA* model was developed using the Green-Ampt equation to represent infiltration (Dussailant et al. 2003; Atchison and Severson 2004) and was recommended to size bioretention facilities in Wisconsin (WDNR 2006). *RECHARGE*, a more comprehensive model for bioretention hydrology, was developed, coupling Richards' equation with a surface water balance as the top boundary condition (Dussailant et al. 2004). Heasom et al. (2006) developed a one-dimensional (1D) hydrological model using HEC-HMS, the Green-Ampt equation, and kinematic wave methods to represent the site and bioretention system, and demonstrated the hydrologic mitigation resulting from implementing bioretention within a small watershed. However, these models

¹Graduate Research Assistant, Dept. of Civil and Environmental Engineering, Univ. of Maryland, College Park, MD 20742. E-mail: zxhe.work@gmail.com

²Professor, Dept. of Civil and Environmental Engineering, Univ. of Maryland, College Park, MD 20742. E-mail: apdavis@umd.edu

Note. This manuscript was submitted on September 2, 2009; approved on July 26, 2010; published online on July 29, 2010. Discussion period open until August 1, 2011; separate discussions must be submitted for individual papers. This paper is part of the *Journal of Irrigation and Drainage Engineering*, Vol. 137, No. 3, March 1, 2011. ©ASCE, ISSN 0733-9437/2011/3-121-131/\$25.00.

are one-dimensional, without describing the horizontal exfiltration into surrounding soils. Meanwhile, limited modeling work is available to show the impacts of common design and site elements on the hydrologic performance of a bioretention cell, which is necessary to assist in creating performance-based bioretention design guidelines.

This work utilizes a two-dimensional (2D) mechanistic model to simulate subsurface flow in a variably saturated bioretention cell, evaluate the hydrologic performance through the underdrain outflow, estimate bottom and side exfiltration into surrounding soils, and examine the effects of some important design parameters or elements, including media, surrounding soils, ratio of drainage area to bioretention surface area, ratio of cell length to width, and initial water content.

Methodology

A 2D variable saturated flow model is developed based on the Richards' equation, which is solved numerically using *COMSOL Multiphysics* (formally *FEMLAB*), a finite-element analysis and solver software (*COMSOL AB 2005*). The subsurface flow fates in bioretention facilities are simulated under unsteady-state conditions. Evapotranspiration is not considered in this model because it is not significant during storm events and can be ignored if a dry or long period is not simulated. All simulations are run at 20°C.

Bioretention Geometry

Fig. 1 shows the 2D geometry of a bioretention cell with width of 3.6 m and height (medium depth) of 0.9 m. The length is assumed as 30 m. The resulting surface area of this cell is 108 m², and the medium volume is 97.2 m³. Water is ponded above the surface layer when the medium is saturated. The height of the ponding space is limited to 0.3 m. The total diameter of the underdrain pipe and its surrounding gravel layer (i.e., the circle within the medium soil subdomain) is 0.3 m, representing a 0.15 to 0.2 m perforated underdrain pipe surrounded by 0.05 to 0.08 m of gravel. The surrounding gravel layer does not go through the entire medium layer, making this underdrain configuration different from an underdrain system with a complete stone layer where largely 1D flow through the medium is expected. Because the boundary conditions between the bioretention medium and surrounding soils (internal boundaries) are unclear, a large modeling geometry is generated by extend-

ing the surrounding soil subdomain for 4.2 m wide on each side and 1.2 m deep under the media. The mulch and vegetated layers are not included in this simple representation.

Governing Equations

The water flow in variably saturated soil is simulated using the Richards' equation, which allows for time-dependent changes in both saturated and unsaturated conditions (Bear 1972, 1979)

$$\frac{(C + SeS)}{\rho_f g} \frac{\partial p}{\partial t} + \nabla \cdot \left[-\frac{K_s}{\rho_f g} k_r \nabla (p + \rho_f g D) \right] = Q_s \quad (1)$$

where C represents specific water capacity (m⁻¹); Se = effective saturation of the soil; S = specific storage with respect to pressure (m⁻¹); ρ_f = fluid density (kg/m³); p = fluid pressure (Pa); t = time (s); K_s = saturated hydraulic conductivity (m/s); k_r = relative hydraulic conductivity; D = vertical coordinate (m); and Q_s represents fluid sources and sinks (s⁻¹).

The soil hydraulic properties θ , C , Se , and k_r change under unsaturated conditions [$H_p = p/\rho_f g < 0$; here H_p is pressure head (m)] and reach a constant value in saturated conditions ($H_p \geq 0$). The liquid volumetric fraction θ ranges from a small value corresponding to the residual liquid volume fraction θ_r to the saturated liquid volume fraction (i.e., porosity) θ_s .

The analytic formulas of van Genuchten are employed to define θ , C , Se , and k_r (van Genuchten 1980). In these expressions, θ , and θ_s as well as constants α , n , l , and m specify the soil type, where $m = 1 - 1/n$

$$\theta = \begin{cases} \theta_r + Se(\theta_s - \theta_r) & H_p < 0 \\ \theta_s & H_p \geq 0 \end{cases} \quad (2)$$

$$C = \frac{\partial \theta}{\partial H_p} = \begin{cases} [(-\alpha m)/(1 - m)](\theta_s - \theta_r) Se^{(1/m)} [1 - Se^{(1/m)}]^m & H_p < 0 \\ 0 & H_p \geq 0 \end{cases} \quad (3)$$

$$Se = \frac{\theta - \theta_r}{\theta_s - \theta_r} = \begin{cases} 1/[(1 + |\alpha H_p|^n)^m] & H_p < 0 \\ 1 & H_p \geq 0 \end{cases} \quad (4)$$

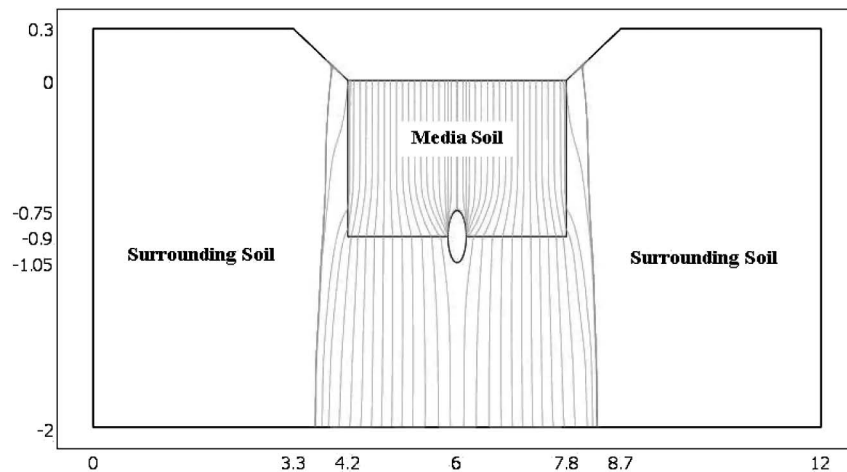


Fig. 1. Geometry of bioretention cell used in the modeling simulations (unit: meters). Note scales are not constant. Streamlines are shown when $t = 0.5$ day for the default storm event

$$k_r = \begin{cases} Se^d \{1 - [1 - Se^{(1/m)}]^m\}^2 & H_p < 0 \\ 1 & H_p \geq 0 \end{cases} \quad (5)$$

Boundary Conditions

The surface boundary of the bioretention medium is crucial, as it is not easy to handle the varying rainfall boundary. Nonsteady-state flow conditions typical of urban storm-water runoff are entered. Specifically, the inflow rate is modeled using a Gaussian function. In the Gaussian function, coefficient \bar{a} is the peak of the inflow, \bar{b} is the time point when the peak inflow velocity appears, and \bar{c} determines the inflow duration, which is assumed to be equal to the rainfall duration. The resulting runoff inflow is given by

$$Q(t) = \bar{a} \exp\left(-\frac{(t - \bar{b})^2}{2(\bar{c})^2}\right) \quad (6)$$

The rational method is used to calculate the peak runoff inflow velocity $v_{in-peak}$

$$v_{in-peak} = ciR_{area} \quad (7)$$

where c = volumetric runoff coefficient, selected as $c = 0.9$ for parking lots (Davis and McCuen 2005); R_{area} = ratio of drainage area to cell surface area, here using $R_{area} = 20$; and i = peak of rainfall intensity.

The storm event for the standard (default) simulation is characterized by a rainfall depth of 1.1 cm and duration of 8.2 h, which is within the range of the second-highest frequency of rainfall events expected in Maryland (0.64–1.27 cm, 7–13 h; Kreeb 2003). This default storm produces outflow, without bypass flow. The highest-frequency rainfalls in Maryland (28%) are short and small storms, which result in no bioretention outflow. The default storm of 1.1 cm is smaller than the Maryland design storm for this cell. To evaluate design parameters, 10 storms (for outflow/inflow volume relationships) or 25 storms (for flow duration curves) are selected according to the expected frequency of rainfall events in Maryland (Kreeb 2003). The storm characteristics selected for simulations are listed in Table 1. The 25 storms simulated for flow duration analysis included all categories with annual frequency larger than 2.21%.

At the underdrain, the water percolating through the media enters the gravel layer, which has high K_s , and then conveys very quickly into the underdrain system through holes in the drainage pipe. The underdrain configuration without a complete stone layer results in differential flow rates through the media, because the flow paths are anisotropic compared with 1D flows that are expected with a typical stone layer. The underdrain pipe must have a hydraulic capacity greater than the maximum media soil-infiltration rate to ensure that the media drains freely (PGC 2007). The boundary condition at the top half circle within the media is set to be atmospheric pressure. However, the bottom half circle, which is placed in the surrounding soil to avoid the formation of a saturation zone in media, is set as no flux.

Infiltration through the sides of the ponding bowl into the surrounding soil is negligible compared with the surface infiltration into the media, because of the smaller bowl side boundaries compared with the media surface boundary and the much lower hydraulic conductivity of the surrounding soils. The system external side boundaries are 4.2 m from the media boundary, 2.3 times the media width. Therefore, the external side boundaries are set to no water flow flux and this lack of system-water loss should not affect flow performance locally in the media. The bottom boundary of the surrounding soils, depth = -2.0 m, is assumed as the groundwater table, with the boundary condition as $H_p = 0$.

Parameters

Hydrologic performances are evaluated by comparing hydrographs, total inflow/outflow volumes, and flow duration curves derived under different bioretention design or site conditions. Flow duration curves are obtained by ranking values of inflow and underdrain flow rate (L/min) for all 25 events, from the highest value to lowest in time increments of 3.6 min.

The default soil textures of the treatment medium and surrounding soil in the standard simulation are a sandy loam and a silt loam, respectively. Model simulations are carried out to test the hydrologic responses to different media surrounded by the same silt loam soil and to the same sandy loam medium surrounded by different soils. Loamy sand and sandy clay loam soils are selected as the alternative media soils. Important hydraulic parameters of the three

Table 1. Ten and 25 Storms Selected Based on Kreeb's Frequency Table of Storm Events for 15 Stations in Maryland

Event-duration (h)	Rainfall-depth (cm)	Frequency % in MD	10 simulated storms			25 simulated storms
			Events	Duration (h)	Depth (cm)	
0–2	0.0254–0.254	28.57	2	1.0, 2.0	0.13, 0.25	7
0–2	0.255–0.635	2.14				1
2–3	0.255–0.635	2.57	1	2.5	0.47	1
2–3	0.636–1.27	2.21				1
3–4	0.255–0.635	2.23	1	3.1	0.56	1
4–7	0.255–0.635	3.51	1	4.0	0.63	1
4–7	0.636–1.27	4.75	2	5.3, 5.6	0.78, 0.95	1
4–7	1.28–2.54	2.21				1
7–13	0.255–0.635	3.37				1
7–13	0.636–1.27	6.29	1	7.2	1.26	2
7–13	1.28–2.54	5.28	1	10	1.91	2
7–13	> 2.54	2.66				1
13–24	0.636–1.27	3.97				1
13–24	1.28–2.54	6.11	1	24	2.54	2
13–24	> 2.54	5.15				1
> 24	> 2.54	4.35				1

Table 2. Hydraulic Parameters of Bioretention Media and Surrounding Soils (Li et al. 1999)

Soil type	K_s [m/day]	θ_s	θ_r	α [m^{-1}]	n^c	l
Media						
Sandy loam ^a	1.063	0.41	0.065	7.5	1.89	0.5
Loamy sand	3.450	0.41	0.057	12.4	2.28	0.5
Sandy clay loam	0.314	0.39	0.10	5.9	1.48	0.5
Surrounding soils						
Silt loam ^b	0.108	0.45	0.067	2	1.41	0.5
Clay loam	0.0624	0.41	0.095	1.9	1.31	0.5
Sandy clay loam	0.314	0.39	0.10	5.9	1.48	0.5

^aStandard soil type of bioretention media.

^bStandard soil type of surrounding soils.

^c $m = 1 - 1/n$.

simulated media and three surrounding soils are listed in Table 2, which are required for the van Genuchten analytical expressions.

The model uses pressure head (H_p) distribution as an initial condition, which is assumed as a linear function of soil depth, since more water is expected to accumulate near the bottom layer than the surface layer of the media because of the much less permeable surrounding soils beneath the media. Initial water content values are integrated over the subdomain of the media by COMSOL post-processing, and the average initial water content (θ_{i-avg}) is calculated for the media soil subdomain. With the default medium and surrounding soil, the impact of initial water content is examined for $\theta_{i-avg} = 0.270, 0.201,$ and 0.165 , corresponding to different initial pressure head distributions.

While keeping the drainage area constant, simulations are run for bioretention cells with different footprint surface areas, but otherwise identical. The area ratios (R_{area}), defined as the ratio of drainage area to bioretention surface area, are 30, 20 (default), and 10.

Bioretention shape is examined while keeping the surface area constant, varying the length-to-width ratio (L/W). The default settings of width and length are 3.6 m and 30 m, respectively ($L/W = 8.33$). For the width equal to 7.2 m, the length is 15 m and $L/W = 2.08$. A single underdrain ($n = 1$) and two underdrains

($n = 2$) are employed in the two wider cells ($W = 7.2$ m), and run along the length of the wider cells ($L = 15$ m).

Mesh

The maximum element size for boundary mesh is 0.02 m at the surface boundary, the top half circle of the underdrain, and at all exfiltration boundaries (internal boundaries). The triangular mesh element sizes in the cell media subdomain are smaller than those in the surrounding soil subdomain because of the computer RAM memory limit, resulting in finer mesh elements with a maximum element size of 0.05 m in the media soil subdomain.

Results and Discussion

Hydrologic Performance

The default bioretention medium is a sandy loam with a saturated hydraulic conductivity, K_s , of 1.06 m/d, surrounded by silt loam soil with smaller K_s of 0.108 m/d. Fig. 2 shows that under the Gaussian distribution influent flow, the peak of the outflow from the underdrain in the default bioretention cell (sandy loam-silt loam) is substantially reduced, from 157 to 13.3 L/min. The time to peak influent from the beginning of influent flow is 0.160 days, while that for the peak effluent is 0.255 days. The total volume of runoff underdrain outflow is 3.89 m³, much less than the inflow volume of 22.7 m³.

Davis (2008) employed three metrics to quantify the hydrologic benefits of two lined-field bioretention facilities in Maryland, including the peak-flow rate ratio of effluent to influent $R_{peak} = q_{peak-out}/q_{peak-in}$, the effluent/influent volume ratio $fV_{24} = V_{out-24}/V_{in}$, and the peak discharge time ratio of effluent to influent $R_{delay} = t_{q-peak-out}/t_{q-peak-in}$. The target fV_{24} value proposed was $fV_{24} < 0.33$ with the same rationale for R_{peak} . In this simulated event, fV_{24} and R_{peak} are 0.171 and 0.085, respectively. The R_{delay} is 1.59. All three of these metrics indicate good hydrologic performance by this bioretention cell.

Simulation results presented in Fig. 3 show the relationship between cumulative underdrain discharge volumes and runoff inflow volumes for 10 storms of various depth and duration

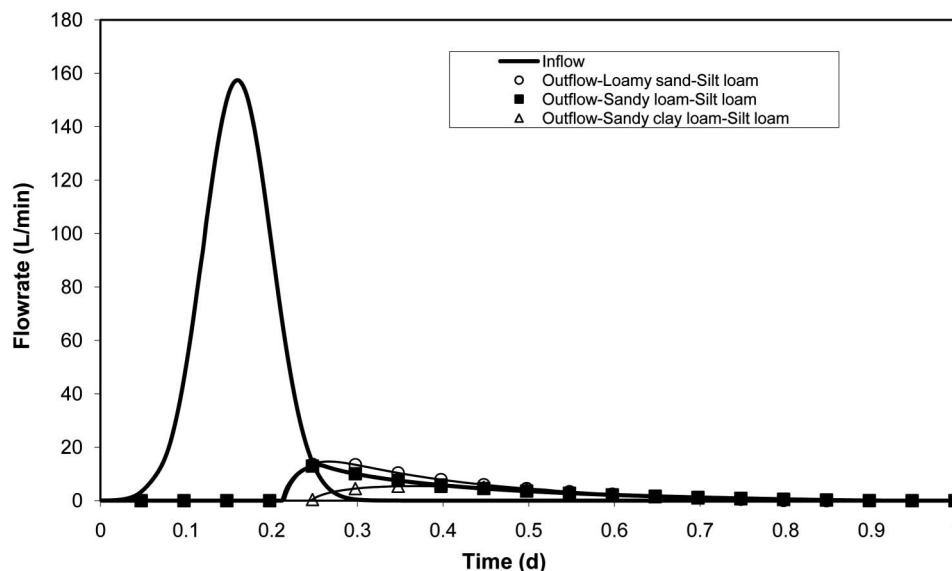


Fig. 2. Inflow and discharge hydrographs for different bioretention media soils responding to the default storm with rainfall depth = 1.1 cm and duration = 8.2 h

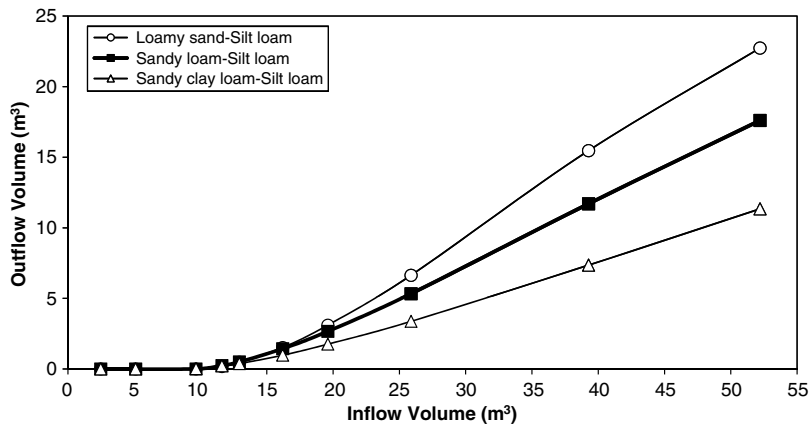


Fig. 3. Relationship between outflow and inflow volumes for different media soils. Ten storm events simulated, as presented in Table 1

(Table 1). Outflow volume is reduced for all 10 events. The default bioretention cell does not produce outflow from the underdrain for storms with runoff inflow volumes $\leq 10 \text{ m}^3$. The storage point is defined as the volume at which the outflow begins. For events that produce inflow volume greater than the storage point, outflow is generated, but the outflow volumes are less than the inflow volumes. Collected bioretention field data also display this trend (Brown et al. 2009). Simulations of 25 storms (Table 1) also show no underdrain flow for small events (rainfall depth less than 0.5 cm). Field study from a 102 m^2 bioretention site in Maryland showed a similar trend, reporting a storage (rainfall) depth of 0.31 cm, using the intercept of a trend line drawn for “zero discharge” events to approximately serve as the boundary between the flow and no-flow events (Li et al. 2009).

Based on the dimensions of the ponding volume, the default bioretention cell can treat at least 40.5 m^3 of inflow runoff without generating bypass flow. For those storms with total inflow runoff volume larger than 40.5 m^3 , it is possible that the bioretention cell will generate bypass flow after the ponding height reaches 0.3 m, especially for conditions of limited media and surrounding soil hydraulic conductivities. Media with high K_s decrease the possibility of bypass flow. Low-intensity rainfall also has a smaller chance to produce bypass flow than high-intensity rainfall even though the total rainfall depths are the same. The bypass flow of extreme storms has not been included in the simulated results.

Parameters

Media Soil Types

Fig. 2 shows the underdrain flow from sandy clay loam, sandy loam (default), and loamy sand media (progressively increasing K_s), surrounded by the same silt loam soil. For the same hydraulic loading, the underdrain outflow characteristics vary for different media types. The sandy clay loam media with lower K_s generates lower discharge flow peak, smaller total discharge volume, and longer lag time to produce peak flow. However, although the K_s of loamy sand is three times higher than that of sandy loam, the lag time for outflow does not differ much for both. This appears to be attributable to the relatively high K_s of these media in comparison with that of the surrounding soil.

Fig. 3 shows the relationship between underdrain discharge volumes and runoff inflow volumes for these three different types of media. For large storms in which all three media produce underdrain outflow, the sandy clay loam medium soil with lower K_s produces smaller total outflow volumes, in agreement with the results in Fig. 2. This is partially because in large storms the medium with

lower K_s more readily produces ponding at the medium surface and allows more time for exfiltration into surrounding soils; however, this ponding also increases the possibility of bypass flow.

The sandy clay loam medium results in a smaller storage point, at an inflow volume of about 7 m^3 , less than the similar storage point of about 10 m^3 for the other two media. Therefore, in some moderate-sized storms, underdrain outflow appears from the sandy clay loam medium, but not from the other two media. The initial effective saturation of sandy clay loam, sandy loam, and loamy sand is 0.75, 0.58, and 0.33, respectively, although the initial pressure head distribution is the same. According to Table 2, the effective porosities ($\theta_s - \theta_r$) are, respectively, 0.280, 0.345, and 0.353. The larger initial effective saturation and smaller effective porosity of the sandy clay loam result in a smaller initial storage capacity as demonstrated in Fig. 3.

Fig. 4 demonstrates a relatively sharp and high inflow duration curve, cumulatively representing the 25 various rainfall events. Also shown are three moderate and low outflow duration curves for three different media types. The sandy clay loam medium has the greatest benefits on reducing the flow. The maximum inflow is 448 L/min. The maximum outflow is 83.7, 41.7, and 17.7 L/min for loamy sand, sandy loam, and sandy clay loam media, respectively. The outflow of the sandy clay loam medium is under 21 L/min for all event time, while that from sandy loam and loamy sand media exceeds 21 L/min for about 1.9 days and 2.5 days, respectively. All three bioretention media reduce the total discharge volume. With the same annual inflow of $586 \text{ m}^3/\text{year}$, the annual outflow is 213, 162, and $97.2 \text{ m}^3/\text{year}$ for loamy sand, sandy loam, and sandy clay loam media, respectively.

Surrounding Soil Types

Fig. 5 shows that, with the same input hydrograph and sandy loam medium, the outflow hydrograph differs for different hydraulic and physical properties of the surrounding soils. Surrounding soils with higher K_s , such as sandy clay loam, generate lower underdrain discharge peaks and smaller total discharge volumes. The peak is also delayed more, although the difference is small. Based on the SWMS 2D model, Li et al. (1999) reported similar results that, for fixed initial effective saturation and decreasing surrounding soil K_s , exfiltration flow from a partial exfiltration trench (PET) tended to decrease and the underdrain outflow increased. Two-dimensional modeling of the PET (VS2DT) by Sansalone and Teng (2005) also supports the results in Fig. 5.

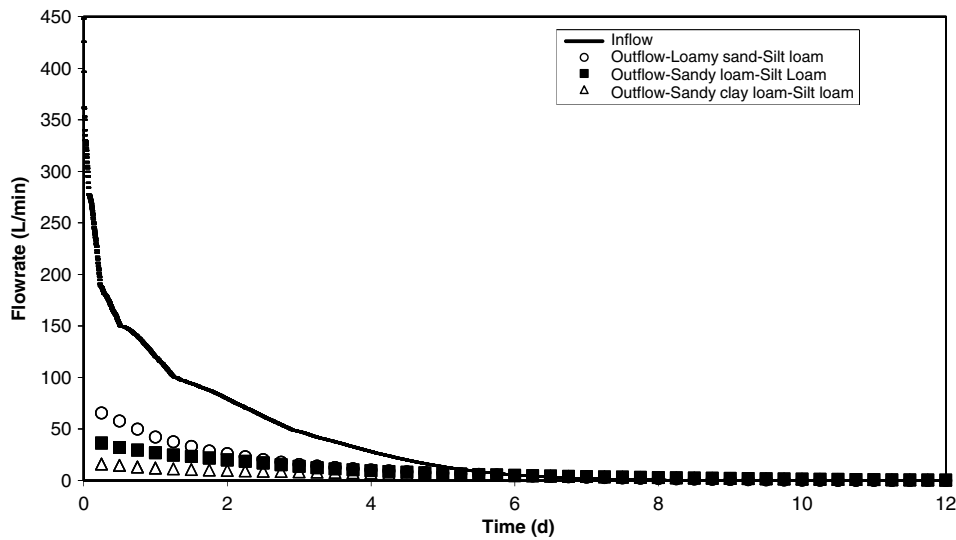


Fig. 4. Flow duration curves for different bioretention media, collected for 25 storms typical in Maryland over one year

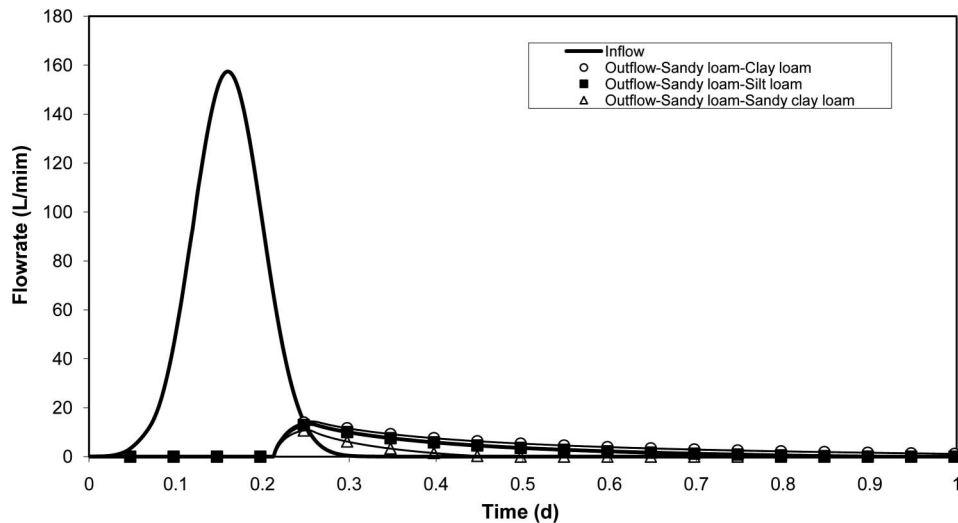


Fig. 5. Inflow and discharge hydrographs for three different surrounding soils responding to the default storm with rainfall depth = 1.1 cm and duration = 8.2 h

Fig. 6 shows the relationship between the discharge and inflow volumes for the default bioretention cell with three different surrounding soils. The storage point for producing outflow appears at a lower volume for clay loam, around 6 m^3 . The storage points for the silt loam and sandy clay loam surrounding soils are 10 and 12 m^3 , respectively. After the storage point, the cell surrounded by a sandy clay loam generates less outflow volume, indicating a significant hydraulic impact for a system with a more permeable surrounding soil. With the same medium type and the same initial pressure head distribution, the initial media storage capacity should be the same. However, the exfiltration into surrounding soils makes an important contribution to the hydrologic mitigation, resulting in the different storage points.

Fig. 7 illustrates the role of different surrounding soil types on the exfiltration into the surrounding soils under influence of the same single storm event. The peak exfiltration flow rate of the sandy clay loam surrounding soil with K_s of 0.314 m/day is two times larger than that of clay loam with K_s of 0.0624 m/day. With the more permeable surrounding soils (larger

K_s), more water enters into surrounding soil layers, resulting in less underdrain effluent discharge from the bioretention cell. The ratio of underdrain flow to inflow is 6.8, 17, and 23% for the system surrounded by sandy clay loam, silt loam, and clay loam, respectively. The corresponding total exfiltration ratio is 87, 64, and 47%, respectively. The difference is temporary storage in the media. Comparing the results in Figs. 5 and 7, for each surrounding soil, the total exfiltration volume is larger than that of underdrain outflow, indicating that the exfiltration into surrounding soils plays an important role in the hydrologic performance.

Further evaluation of exfiltration flows shows that, for each of the three surrounding soils, the exfiltration flow from the bottom of the bioretention cell is the primary component of the total exfiltration flow, much larger than that from the sides. Bottom exfiltration accounts for 88–95% of total exfiltration. The lowest curve in Fig. 7 shows the bottom exfiltration flow into the clay loam surrounding soil, amounting to about 88% of the total exfiltration flow volume. The bottom exfiltration flow will eventually enter the groundwater

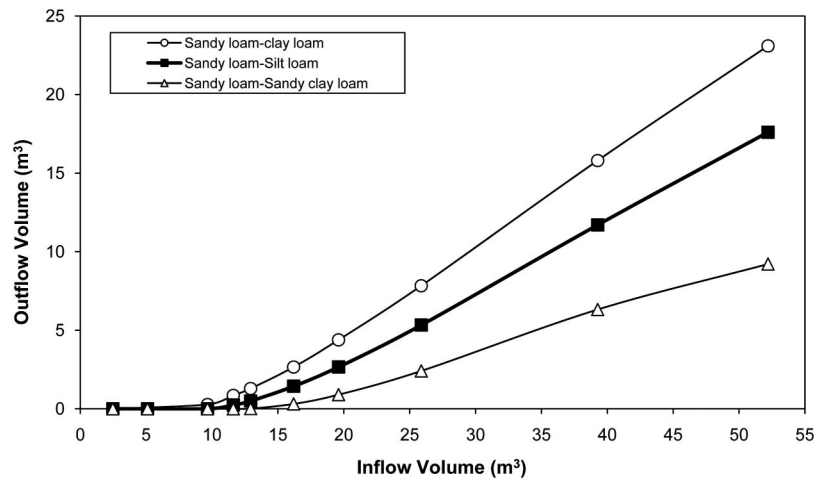


Fig. 6. Relationship between outflow and inflow volumes for different surrounding soils. Ten storm events simulated, as presented in Table 1

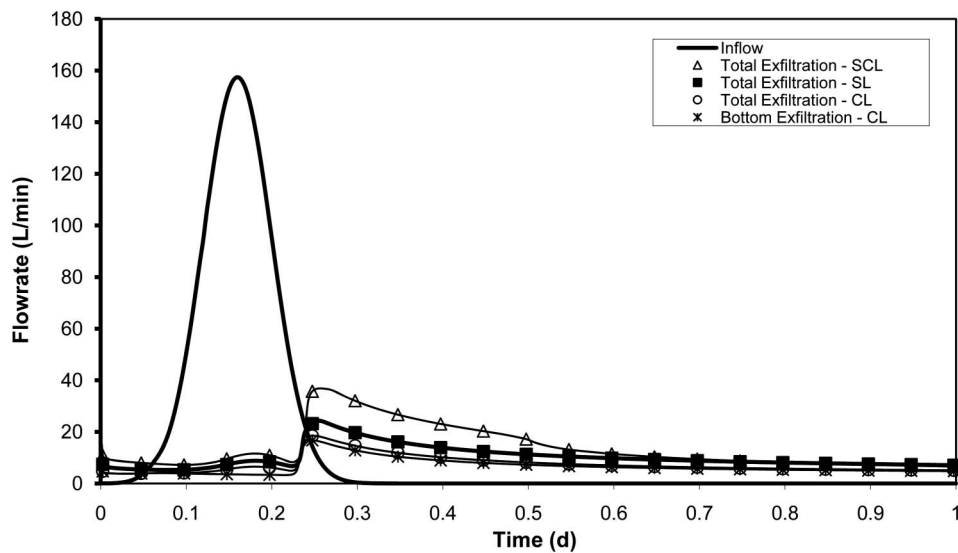


Fig. 7. Inflow and total exfiltration flow into three different surrounding soils, responding to the default storm. The lowest curve is the bottom exfiltration flow into the clay loam surrounding soil

system and has the potential to increase the base flow of streams and promote healthy aquatic ecosystems.

Initial Water Content

Fig. 8 shows the hydrograph impact of the initial bioretention media water content, represented by θ_{i-avg} . Under the default settings ($\theta_{i-avg} = 0.270$), the total outflow volume is larger, with higher peak flow and less lag time to peak than the other two simulations. Under drier conditions, when the average initial water content is reduced to 0.165, the total outflow is close to zero. For comparison, Barber et al. (2003) modeled the hydrologic performance of an ecology ditch, a similar infiltration BMP, and found that small changes in the initial water content had significant effects on the hydrologic performance in small events. Muthanna et al. (2008) studied two small-scale rain gardens in a cold-climate coastal area in Norway, and found that the hydrologic performance was strongly related to temperature and antecedent water content (time since last event). The lag time (defined as time for outflow to occur) showed a strong positive correlation with the length of antecedent dry period.

The relationship between outflow and inflow volume in Fig. 9 demonstrates a significantly larger storage point for smaller average initial water contents. The drier soil ($\theta_{i-avg} = 0.165$) attenuates the entire volume for the seven smallest events, while the wetter soil ($\theta_{i-avg} = 0.270$) completely attenuates only three entire events out of 10.

Higher initial water content consumes greater initial storage, providing less storage capacity to absorb runoff, and therefore produces earlier outflow and larger total discharge volume. A typical antecedent dry weather period of an area should be considered when designing and evaluating hydrologic performance of a bioretention facility. In wet seasons and in winter with associated lower evapotranspiration, an increase in saturation or in groundwater level contributes to an increase in initial soil water content and will affect the bioretention performance.

Bioretention Area Ratios

Fig. 10 shows the hydrographs when the drainage to bioretention surface area ratio (R_{area}) is 30, 20, and 10. All three improve hydrologic performance over the input. As expected, the peak flow and

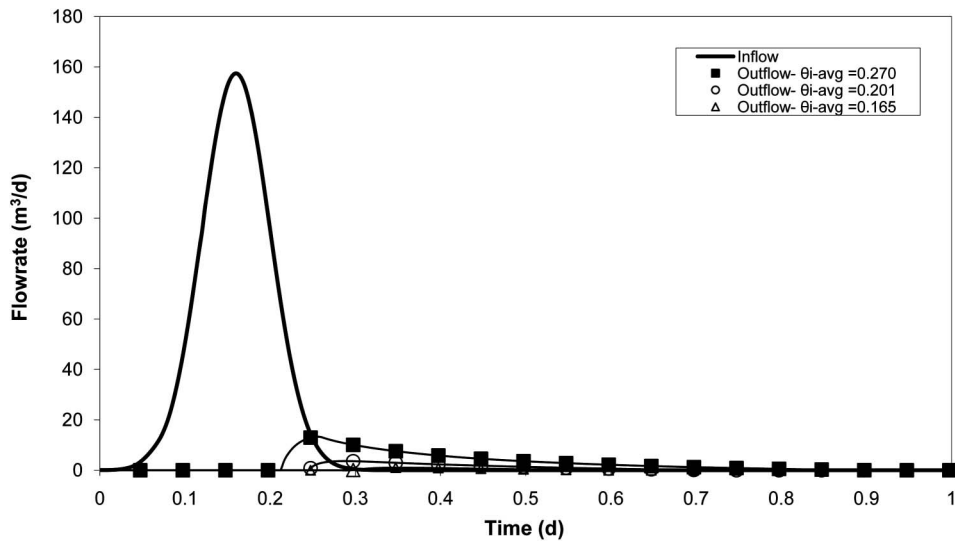


Fig. 8. Inflow and discharge hydrographs for different average initial water contents, responding to the default storm

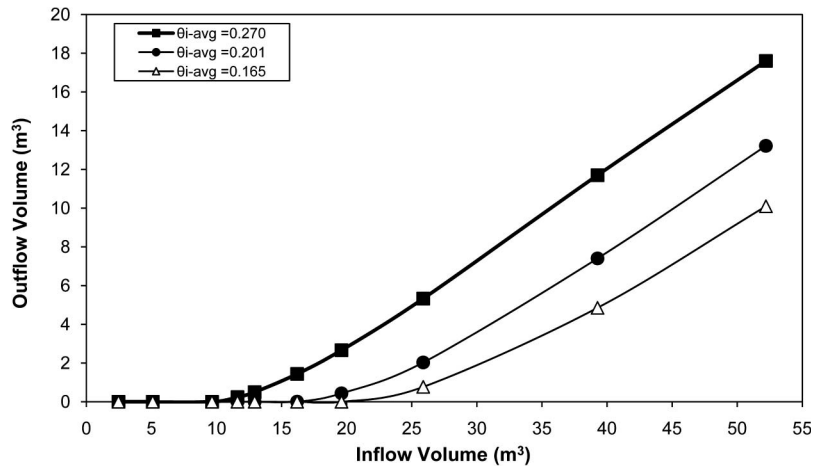


Fig. 9. Relationship between outflow and inflow volumes for different average initial water contents. Ten storm events simulated, as presented in Table 1

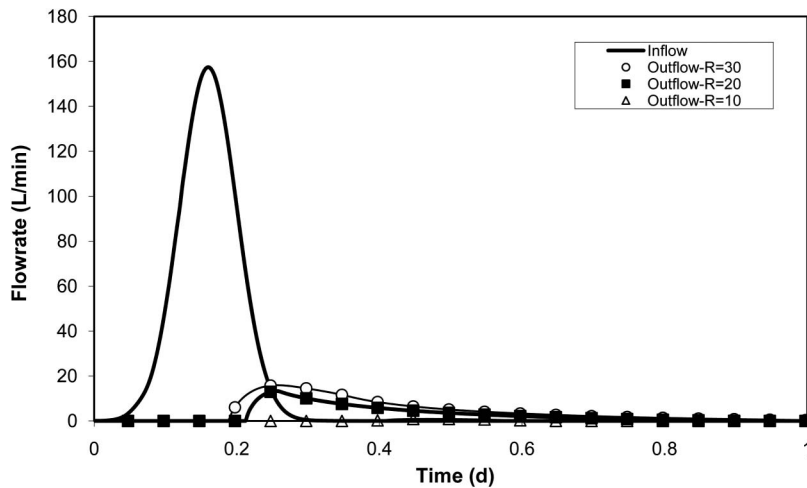


Fig. 10. Inflow and discharge hydrographs for different ratios of drainage area to bioretention area, responding to the default storm

total outflow volume is larger when the area ratio R_{area} is larger. Reducing the area ratio to 10 produces an outflow for the default event that is close to zero.

Fig. 11 clearly demonstrates that the larger-sized bioretention cells (with smaller R_{area}) have better hydrologic performance than smaller-sized cells. A facility sized at 10% of the drainage area ($R_{\text{area}} = 10$) can completely assimilate storms with rainfall depths less than approximately 1.13 cm over the drainage area without generating underdrain flow. The 3.33%-sized cell ($R_{\text{area}} = 30$) can only absorb the entire storm runoff for rainfall depths less than about 0.26 cm.

The larger-sized bioretention cell improves the performance because of the increased pool and media (pore) storage volume. Li et al. (2009) monitored the hydrologic performance of six bioretention cells with different surface areas and media depths in Maryland and North Carolina, and reported that a larger media volume to drainage area ratio appears to improve the performance, in agreement with the results in Figs. 10 and 11. The typical ratio of drainage area to bioretention area is 20 (the standard setting in these simulations) to 40. In addition to a higher peak and total outflow

volume, a high area ratio may also result in rapid water pooling and greater bypass flow during moderate rainfall events. However, a low area ratio increases the cost of land, installation, and maintenance. Therefore, a balance among typical hydraulic loading, hydrologic performance, and cost must be considered when designing a bioretention facility.

Bioretention Cell Widths

Fig. 12 shows that a wider cell with two underdrain pipes ($W = 7.2$ m and $n = 2$) and the standard cell ($W = 3.6$ m and $n = 1$) have the same outflow curve for the default storm (the curves overlap). Similarly, Fig. 13 shows that the volumetric performances are identical when inflow volume is less than 20 m^3 . In Fig. 12, the outflow volume of the wider cell with one underdrain ($W = 7.2$ m and $n = 1$) is less, with a lower peak.

The storage points of discharge are approximately the same for all designs (Fig. 13). All three cells can absorb the entire storm runoff for rainfall depth less than 0.56 cm. Therefore, these cells have the same storage capability to treat smaller storms, because of the nearly identical media volume (the underdrain and gravel occupy only up to 1% of the total media volume). Fig. 13 shows

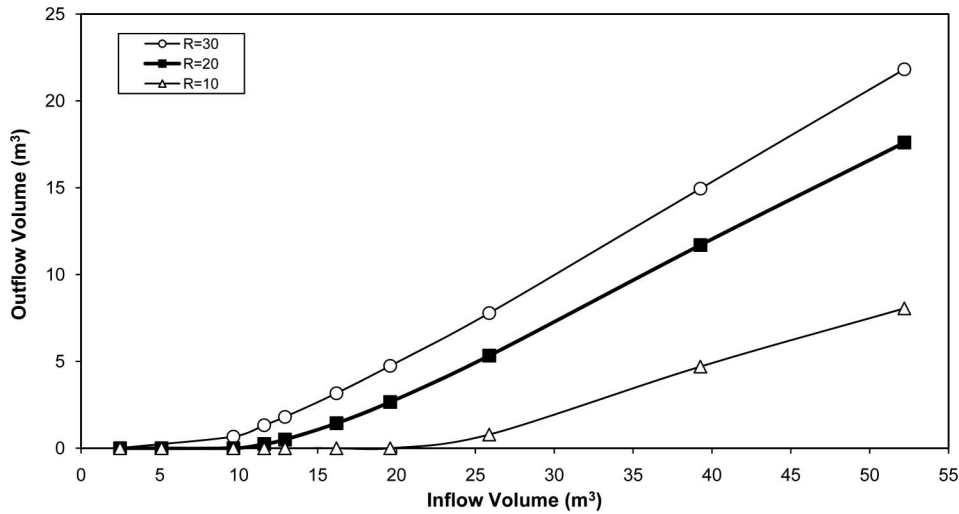


Fig. 11. Relationship between outflow and inflow volumes for different ratios of drainage area to bioretention area. Ten storm events simulated, as presented in Table 1

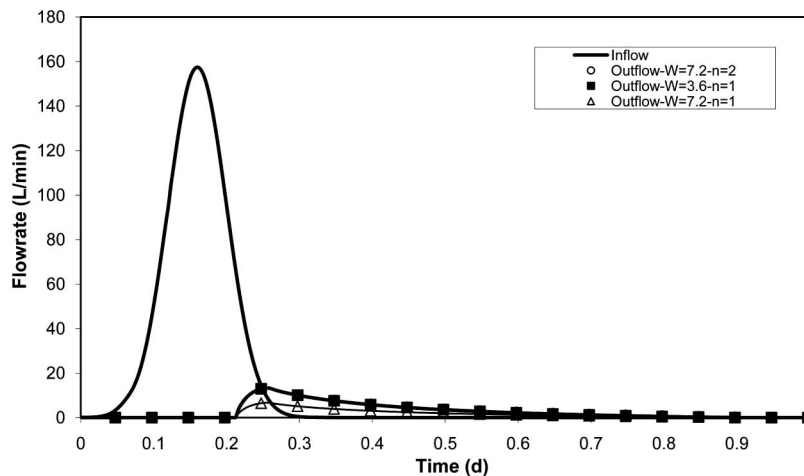


Fig. 12. Inflow and discharge hydrographs for different widths in the same surface area of a bioretention cell and different number of underdrain pipes, responding to the default storm

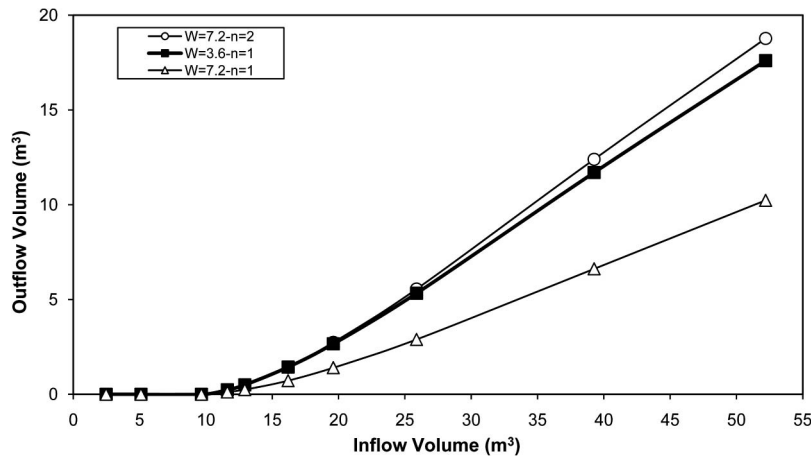


Fig. 13. Relationship between outflow and inflow volumes for different widths with the same cell surface area and different number of underdrain pipes. Ten storm events simulated, as presented in Table 1

larger volumetric discharge for a wider cell with two underdrains ($W = 7.2$ m and $n = 2$), compared with an identical cell with one underdrain ($W = 7.2$ m and $n = 1$), for the default storm. In the case of two cells of the same shape, the side exfiltration areas are the same. However, according to the streamlines in Fig. 1, the underdrain (and the gravel layer) demonstrates a flow-pattern impacting zone, within which the water will be collected by the underdrain system. Water beyond this zone, too far from the underdrain, will exfiltrate through the media bottom into the surrounding soils. The wider cell with one underdrain only has one impacting zone, resulting in larger bottom exfiltration than the wider cell with two underdrains, which funnel water from nearly all of the media. A cell having a complete stone layer may lessen the noted impacts of underdrain configuration.

The wider cell with two underdrains ($W = 7.2$ m and $n = 2$) produces slightly larger discharge volume than the standard cell ($W = 3.6$ m and $n = 1$) under the same simulated larger storms. The wider cell has two underdrain impacting zones, although its width is double, so the bottom exfiltration flows are approximately the same in these cells. However, the larger total side-wall surface area in the standard cell increases the horizontal exfiltration from the four sides, assuming that exfiltration rates through the four side walls are the same. Therefore, a narrow cell (same surface area and total underdrain length) appears to improve the hydrologic performance for larger storms.

A length to width ratio of at least 2 is generally recommended for bioretention design. According to the simulated results, this ratio may not affect the treatment for small storms. However, a higher length to width ratio may improve the hydrologic performance for large storms. It appears also that underdrain number and positioning are important to performance.

Conclusions

In this study, a 2D variable saturated flow model to describe storm-water runoff in a bioretention cell is developed based on the Richards' equation application mode in COMSOL Multiphysics. This model is tested under transient hydraulic loading. Model results semiquantitatively match field results for a number of hydrologic metrics. The outflow volume is always less than the inflow. Discharge flow rates are reduced and delayed. The bioretention cell generates no underdrain flow for small storms.

Simulated results show that the saturated hydraulic conductivity, storage capacity, and exfiltration into surrounding soils contribute to the improved hydrologic performance of a bioretention cell:

1. Underdrain outflow volume from a finer medium with smaller K_s (such as sandy clay loam) is less than that from a coarser medium because in large storms the less-permeable medium more readily produces ponding at the media surface and, correspondingly, allows greater time for exfiltration. However, this also increases the possibility of bypass flow. This study does not include the results of bypass flow, which is expected to occur for a small fraction of the storm events evaluated;
2. Initial media storage capacity is affected by the hydraulic properties of the media, initial water content, and media volume. A sandy clay loam medium with smaller effective porosity generates a smaller (or earlier) breakthrough storage point for underdrain discharge. A medium with higher initial water content produces an earlier outflow and larger total discharge volume. When the ratio of drainage area to bioretention area (R) decreases, the larger-sized bioretention cell improves the hydrologic performance;
3. Exfiltration into surrounding soils can play an important role in the attenuation of storm-water runoff. Surrounding soils with larger K_s produce less outflow volume than those with smaller K_s values. Exfiltration through the bottom is predominant over that through the sides. With the same media surface area and underdrain length, the outflow volume increases slightly with an increase in width, attributable to a decrease in the total wall area for horizontal exfiltration.

Different soil types with different hydraulic properties in both the media and surrounding soils greatly affect the underdrain outflow from a bioretention cell. Careful consideration of the soil types of both is important in selecting the design and function of a bioretention cell. Media with lower K_s values will reduce outflow rates and total volume. However, this less-permeable soil will more easily generate surface pooling, which should be maximized to limit subsequent overflow and bypass. A smaller ratio of drainage area to bioretention area (a larger-sized cell) will produce better resulting hydrologic performance. When selecting the area ratio, a balance among the typical hydraulic loading, hydrologic performance, and cost should be considered. When the bioretention surface area is fixed, a long and narrow bioretention cell will provide improved performance in the treatment of large storms. The specification of specific hydrologic metrics and goals will allow

quantitative prediction of bioretention performance and lead to specific design specifications.

Acknowledgments

This research was supported by TATE Incorporated, Germantown, Maryland.

References

- Atchison, D., and Severson, L. (2004). *RECARGA user's manual, version 2.3*. Univ. of Wisconsin–Madison, Civil & Environmental Engineering Dept., Water Resources Group, Madison, WI.
- Barber, M. E., King, S. G., Yonge, D. R., and Hathhorn, W. E. (2003). “Ecology ditch: A best management practice for storm water runoff mitigation.” *J. Hydrol. Eng.*, 8(3), 111–122.
- Bear, J. (1972). *Dynamics of fluids in porous media*, Elsevier Scientific, New York.
- Bear, J. (1979). *Hydraulics of groundwater*, McGraw-Hill, New York.
- Brown, R. A., Hunt, W. F., Davis, A. P., Traver, R. G., and Olszewski, J. M. (2009). “Bioretention/bioinfiltration performance in the mid-Atlantic.” *ASCE World Environmental and Water Resources Congress 2009*, Kansas City, MO.
- COMSOL AB (2005). *COMSOL Multiphysics earth science module user's guide* (version 3.2).
- Davis, A. P. (2008). “Field performance of bioretention: Hydrology impacts.” *J. Hydrol. Eng.*, 13(2), 90–95.
- Davis, A. P., Hunt, W. F., Traver, R. G., and Clar, M. E. (2009). “Bioretention technology: An overview of current practice and future needs.” *J. Environ. Engrg. Div.*, 135(3), 109–117.
- Davis, A. P., and McCuen, R. M. (2005). *Stormwater management for smart growth*, Springer, New York.
- Delaware Natural Resources and Environmental Control (DNREC). (2005). *Green technology: The Delaware urban runoff management approach*, Delaware Dept. of Natural Resources and Environmental Control, Division of Soil and Water Conservation, Dover, DE.
- Dietz, M. E., and Clausen, J. C. (2005). “A field evaluation of rain garden flow and pollutant treatment.” *Water, Air, Soil Pollut.*, 167(1–4), 123–138.
- Dussaillant, A. R., Cozzetto, K., Brander, K., and Potter, K. W. (2003). “Green-Ampt model of a rain garden and comparison to Richard's equation model.” *Sustainable planning and development, the sustainable world*, WIT Press, Southampton, UK, 891–900.
- Dussaillant, A. R., Wu, C. H., and Potter, K. W. (2004). “Richard's equation model of a rain garden.” *J. Hydrol. Eng.*, 9(3), 219–225.
- Heasom, W., Traver, R. G., and Welker, A. (2006). “Hydrologic modeling of a bioinfiltration best management practice.” *J. Am. Water Resour. Assoc.*, 42(5), 1329–1347.
- Hunt, W. F., Jarrett, A. R., Smith, J. T., and Sharkey, L. J. (2006). “Evaluating bioretention hydrology and nutrient removal at three field sites in North Carolina.” *J. Irrig. Drain Eng.*, 132(6), 600–608.
- Kreeb, L. B. (2003). “Hydrologic efficiency and design sensitivity of bioretention facilities.” Honors Research, Univ. of Maryland, College Park, MD.
- Li, H., Sharkey, L., Hunt, W. F., and Davis, A. P. (2009). “Mitigation of impervious surface hydrology using bioretention in North Carolina and Maryland.” *J. Hydrol. Eng.*, 14(4), 407–415.
- Li, Y., Buchberger, S. G., and Sansalone, J. J. (1999). “Variably saturated flow in storm-water partial exfiltration trench.” *J. Environ. Eng.*, 125(6), 556–565.
- Maryland Dept. of the Environment (MDE). (2000). *2000 Maryland storm-water design manual, vols. I & II*, MDE, Baltimore.
- Muthanna, T. M., Viklander, M., and Thorolfsson, S. T. (2008). “Seasonal climatic effects on the hydrology of a rain garden.” *Hydrol. Processes*, 22(11), 1640–1649.
- PGC. (2007). *Bioretention manual*, Prince George's County, Maryland, Dept. of Environmental Resources, Environmental Services Division, Landover, MD.
- Sansalone, J. J., and Teng, Z. (2005). “Transient rainfall-runoff loadings to a partial exfiltration system: Implications for urban water quantity and quality.” *J. Environ. Eng.*, 131(8), 1155–1167.
- WDNR. (2006). “Bioretention for infiltration.” *Rep. No. 1004*, Wisconsin Dept. of Natural Resources, Madison, WI.
- van Genuchten, M. T. (1980). “A closed-form equation for predicting the hydraulic conductivity of unsaturated soils.” *Soil Sci. Soc. Am. J.*, 44(5), 892–898.
- Yang, H., Florence, D. C., McCoy, E. L., Dick, W. A., and Grewal, P. S. (2009). “Design and hydraulic characteristics of a field-scale bi-phasic bioretention rain garden system for stormwater management.” *Water Sci. Technol.*, 59(9), 1863–1872.